



Title	Cathodoluminescence from interband transitions in germanium (111) and gallium arsenide (100) crystals
Author(s)	Xu, XL; Hao, LY; Xu, KZ; Chen, TP; Fung, S
Citation	Physical Review B, 1995, v. 52 n. 3, p. 1452-1455
Issued Date	1995
URL	http://hdl.handle.net/10722/43438
Rights	Physical Review B (Condensed Matter). Copyright © American Physical Society.

Cathodoluminescence from interband transitions in germanium (111) and gallium arsenide (100) crystals

X. L. Xu

Department of Physics, University of Hong Kong, Pokfulam Road, Hong Kong

L. Y. Hao and K. Z. Xu

Department of Modern Physics, University of Science and Technology of China, Hefei, Anhui 230026, People's Republic of China

T. P. Chen and S. Fung

Department of Physics, University of Hong Kong, Pokfulam Road, Hong Kong

(Received 9 August 1994; revised manuscript received 3 February 1995)

The cathodoluminescence spectra in *n*-type Ge(111) and semi-insulating (SI) GaAs(100) were measured in the range 2.20–5.20 eV. We observed five structures at 3.05, 3.22, 3.60, 3.90, and 4.30 eV in *n*-type germanium which are assigned to interband transitions. These results are similar to those of previous works on *p*-type Ge(111). For SI GaAs, the five structures observed at 2.95, 3.26, 3.88, 4.28, and 4.96 eV also indicate electron-hole recombination transitions between bands. All these results agree with the predictions of theoretical calculations. For lightly doped germanium, it is observed that the band structure does not depend on doping type.

Cathodoluminescence (CL) of interband transition is the recombination of electrons from the conduction band and holes from the valence band across the fundamental energy gap. To determine the band structure of a semiconductor, it is important to study the optical transitions in a wide energy region (1–10 eV) above the intrinsic threshold. Over the past two decades, a number of experimental tools have become available for investigating the electronic band structure of semiconductors. For instance, various photoemission spectroscopy techniques, i.e., x-ray photoemission¹ and ultraviolet photoemission² have been developed. Previous CL experiments^{2–10} and theoretical calculations¹¹ have shown that the CL spectra of all semiconductors are in the region of wavelength near that corresponding to the fundamental absorption edge. The band structures of a series of semiconductors

have been successfully calculated using “the local”¹² and “the nonlocal”^{13,14} empirical pseudopotential method (EPM). The band structures of Ge and GaAs are shown in Fig. 1 and the eigenvalues at Γ , X , and L are tabulated in Table I.

Ge is an indirect-gap semiconductor. The probability of optical transitions in such a material is significantly lower as compared with that process in a direct-gap semiconductor, such as GaAs. However, optical emission bands can be “activated” by impurity or defect atoms called “activator.”¹⁵ Emission spectra which depend on the presence of impurities generally have much greater intensities than those in a pure material. Sernelius¹⁶ reported some band shifts in heavily doped *n*- and *p*-type semiconductors. Thus, for our present measurements, we use lightly doped *n*-type Ge. As for GaAs, semi-insulating (SI) materials were selected for our samples.

We have previously reported the photoemission spectra of *n*-type Si (111) excited by a ⁹⁰Sr β source¹⁷ and that of CL spectra of *p*-type Ge (111) (Ref. 18) measured at room temperature. In this work, the CL spectra of *n*-type Ge (111) and SI GaAs were measured under the same experimental conditions.

Table II describes the two samples used in this work. The value of resistivity of Ge was fairly large, indicating that the samples were lightly doped; the impurity concentration was around 10^{15} cm^{-3} .¹⁹

CL spectra were obtained at room temperature using a 0.3 m monochromator with a grating blazed at 350 nm and a XP2020Q photomultiplier. The schematic diagram of the electron-gun system is shown in Fig. 2. The intensity of the electron current on the target was 10^{-6} A/cm^2 , with an energy of 4 keV. There was a liquid-nitrogen trap between the chamber and the turbo pump. The working pressure in the system was 10^{-5} Pa . A magnetic coil was used to deflect the electron beam in order to prevent the direct light from the filament from illuminating the target. The resolutions of the monochromator were 1 nm for Ge and 1.5 nm for SI GaAs. The

TABLE I. Eigenvalues for Ge and GaAs at Γ , X , and L (Ref. 13) energies are in eV. (The data in brackets are from Ref. 14.)

Point	Level	Compound	
		Ge	GaAs
Γ	7V	-0.29 (-0.28)	-0.35 (-0.33)
	8V	0.00 (0.00)	0.00 (0.00)
	6C		1.51 (1.53)
	7C	0.90 (1.00)	4.55 (3.90)
	6C	3.10 (3.03)	
	8C	3.22 (3.27)	4.71 (4.17)
X	6V		-2.99 (-2.32)
	7V		-2.89 (-2.22)
	5V	-3.29 (-2.70)	
	5C	1.16 (1.19)	
	6C		2.03 (2.40)
	7C		2.38
L	6V	-1.63 (-1.45)	-1.42 (-1.15)
	4,5V	-1.43 (-1.23)	-1.20 (-0.92)
	6C	0.76 (0.77)	1.82 (2.26)
	6C	4.16	5.47 (4.95)
	4,5C	4.25	5.52

CL spectra of Ge measured in the energy range from 2.40 to 4.60 eV are shown in Fig. 3, and those of GaAs measured from 2.20 to 5.20 eV are shown in Fig. 4. All probable transitions are listed in Table III.

The reasons for the difference in the values between measurement and theoretical calculations are twofold. One problem could be systematic; for example, apparatus resolution, energy and intensity of input electrons, radiation time, and so on. Second, the discrepancy could come from the chosen method of calculation. In an earlier publication,¹⁸ we discussed the effect of incident electrons on the target. This distorts the bands of free electrons and smoothes the Van Hove singularities, which leads to a decrease in photon emission and the occurrence of new structures. As a matter of fact, the density of states near the Van Hove singularities is too large to be smoothed rapidly, and thus, for a certain measurement duration, the observed transitions corresponding to these singularities still retain the peak emission features, such as peak intensity and width. Figure 5 shows the comparison of electron-photon emission spectra at different times and different energies and intensities of the input electrons. The measurement time of getting a whole spectrum is about half an hour. We have obtained the

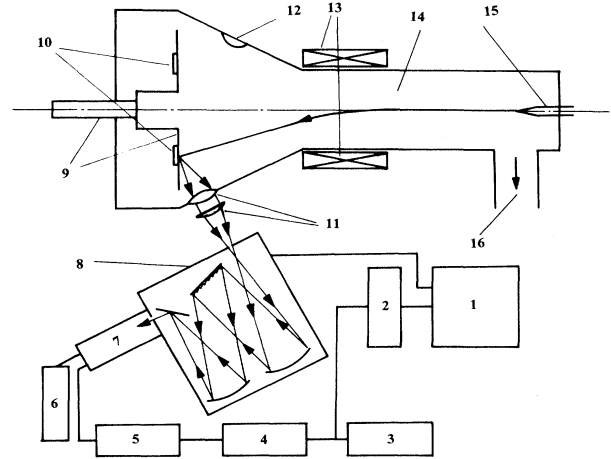


FIG. 2. Schematic diagram of an electron-gun system. 1, computer; 2, analog-digital converter (ADC); 3, counter; 4, single-channel analyzer; 5, amplifier; 6, high-voltage source; 7, XP2020Q photomultiplier; 8, monochromator; 9, rotational sample frame; 10, samples; 11, lens; 12, observation window; 13, magnetic deflection coils; 14, vacuum chamber; 15, filament; 16, pumping.

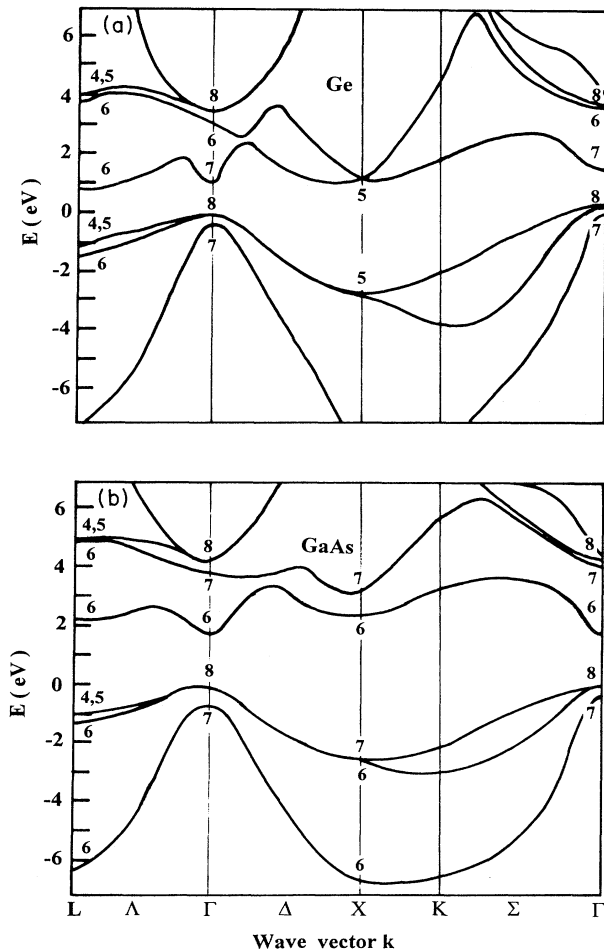


FIG. 1. (a) Germanium band structure and (b) gallium arsenide band structure calculated by EPM (Refs. 4 and 5).

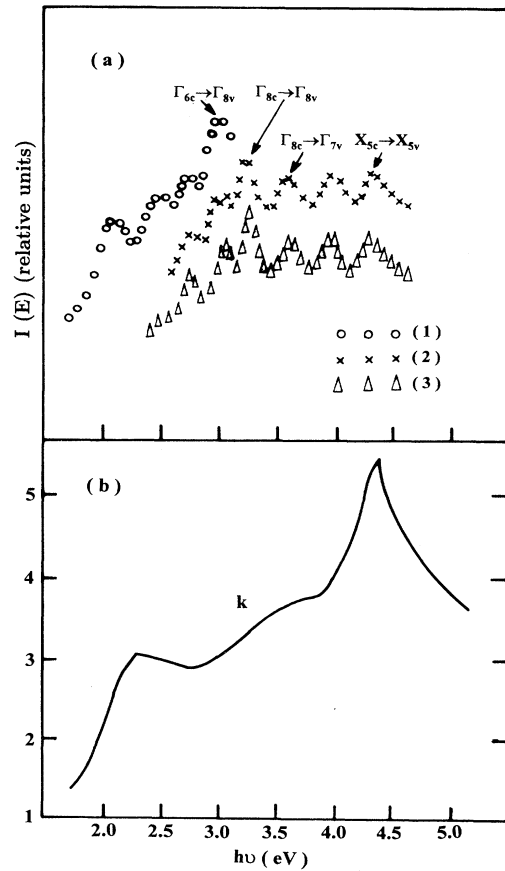


FIG. 3. (a) CL spectra of (1) polycrystalline Ge obtained for $E_p = 200$ eV (Ref. 20), (2) *p*-type Ge (111) (Ref. 18), and (3) *n*-type Ge (111). (b) Extinction coefficient *k*.

TABLE II. Characteristics of two samples.

Samples	Orientation	Resistivity	Surface clean by
<i>n</i> -type germanium	(111)	0.92–1.06 Ω cm	hydrofluoric acid
SI gallium arsenide	(100)	~10 ⁸ Ω cm	No. 2 solution ^a

^aThe formula of the number 2 solution is HCL:H₂O₂:H₂O=1:2:8.

spectra with the smallest distortion at energy $E_i = 2$ keV, intensity $I_i = 10^{-6}$ A/cm², and $E_i = 4$ keV, $I_i = 10^{-7}$ A/cm² [see Fig. 5(c) and 5(e)]. However, under these conditions, the statistical errors are quite large, because of the lower counting rates. There is some spectral distortion when $E_i = 4$ keV and $I_i = 10^{-6}$ A/cm², but the peak positions can still be distinguished clearly; and thus higher counting rates with lower statistical error were also used. For these reasons, we took 4 keV and 10^{-6} A/cm² to be the energy of intensity of input electrons. To avoid distortion of the spectra by the irradiation effect and to minimize any distortion present, we also measured the spectrum of each peak, respectively, in order to shorten each time of measurement. Before each new set of data was collected (within 5 min), our sample shelf was

TABLE III. The CL transitions (Ref. 13) in Ge and GaAs, energies are in eV. (Transitions in brackets are from Ref. 14.)

Samples	CL energies		Transitions
	experimental	theoretical	
Ge(111)	3.05±0.03	(3.03) 3.10	($\Gamma_{6c} \rightarrow \Gamma_{8v}$) $\Gamma_{6c} \rightarrow \Gamma_{8v}$
	3.22±0.03	3.22 (3.27)	$\Gamma_{8c} \rightarrow \Gamma_{8v}$ ($\Gamma_{8c} \rightarrow \Gamma_{8v}$)
	3.60±0.04	3.55 (3.51)	($\Gamma_{8c} \rightarrow \Gamma_{7v}$) ($\Gamma_{8c} \rightarrow \Gamma_{7v}$)
	3.90±0.05	(3.89)	($X_{5c} \rightarrow X_{5v}$)
	4.30±0.07	4.45	$X_{5c} \rightarrow X_{5v}$
GaAs(100)	2.95±0.04	3.02	$L_{6c} \rightarrow L_{4,5v}$
	3.26±0.04	3.22 (3.41)	$L_{6c} \rightarrow L_{6v}$ ($L_{6c} \rightarrow L_{4,5v}$)
	3.88±0.08	3.90	($\Gamma_{7c} \rightarrow \Gamma_{8v}$)
	4.28±0.08	(4.23, 4.17)	($\Gamma_{7c} \rightarrow \Gamma_{7v}$, $\Gamma_{8c} \rightarrow \Gamma_{8v}$)
	4.96±0.10	4.90, 5.03, 4.93	$\Gamma_{7c} \rightarrow \Gamma_{7v}$, $X_{6c} \rightarrow X_{6v}$
			$\rightarrow X_{6v}$, $X_{6c} \rightarrow X_{7v}$

rotated so that the electron beam was always incident on a fresh surface of the samples.

In contrast with the results of *p*-type Ge, we obtained the same structures in *n*-type Ge, but without energy shifts for every peak position. This indicates that there is no appreciable change on the band structure of the lightly doped semiconductor (*p*-type Ge was also lightly doped). Thus, when investigating the band structure of a semiconductor, it would seem more useful to study ex-

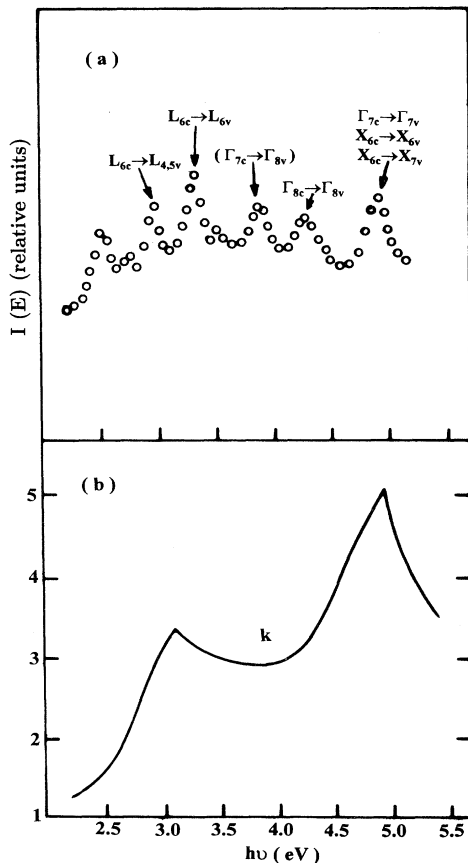


FIG. 4. (a) CL spectrum of GaAs, (b) extinction coefficient k .

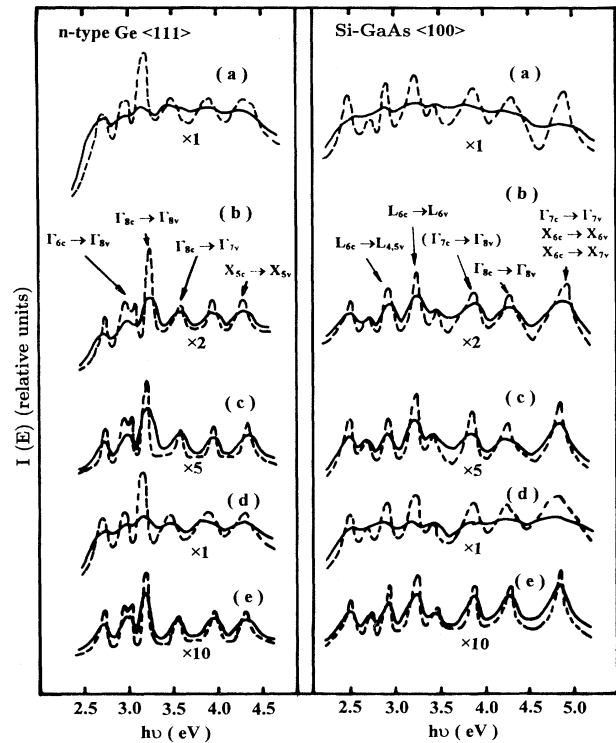


FIG. 5. The comparison of CL spectra at different times. The full curve shows the spectra measured after an extra 30 min of irradiation time (E_i : energy of input electrons, I_i : intensity of input electrons). (a) $E_i = 8$ keV, $I_i = 10^{-6}$ A/cm²; (b) $E_i = 4$ keV, $I_i = 10^{-6}$ A/cm²; (c) $E_i = 4$ keV, $I_i = 10^{-7}$ A/cm²; (d) $E_i = 4$ keV, $I_i = 10^{-5}$ A/cm²; (e) $E_i = 2$ keV, $I_i = 10^{-6}$ A/cm².

trinsic samples with an appropriate impurity concentration rather than studying the corresponding pure material. The three structures at 3.05, 3.22, and 3.60 eV are in agreement with the results of calculations by both Refs. 13 and 14. According to these calculations, the structures are corresponding to the transitions $\Gamma_{6c} \rightarrow \Gamma_{8v}$, $\Gamma_{8c} \rightarrow \Gamma_{8v}$, and $\Gamma_{8c} \rightarrow \Gamma_{7v}$. The 3.90 and 4.30 eV structures are fitted to the $X_{5c} \rightarrow X_{5v}$ transition in Refs. 13 and 14. These are listed in Table III.

For the SI GaAs samples, to avoid the charge accumulation effect, we selected a copper net (whose CL spectrum is known) to cover the surface of the sample. With this work, we obtained the CL spectra in the energy region from 2.20 to 5.20 eV. Five structures located at 2.95, 3.26, 3.88, 4.28, and 4.96 eV are fitted, respectively, to the transitions of $L_{6c} \rightarrow L_{4,5v}$, $L_{6c} \rightarrow L_{6v}$, $\Gamma_{7c} \rightarrow \Gamma_{8v}$, $\Gamma_{8c} \rightarrow \Gamma_{8v}$, $\Gamma_{7c} \rightarrow \Gamma_{7v}$ and so on. These have also been listed in Table III.

To facilitate easier comparison, the values of the extinction coefficient k (Refs. 21–23) are shown in both Figs. 3 and 4. The CL spectra of Ge and GaAs indicate that some of these peaks are present in the regions, where k decreases rapidly. In general, large changes of absorption would produce some peak shifts. However, in the spectral region of our measurements, the semiconductors strongly absorb photons, having coefficients of absorption of the order of 10^5 – 10^6 cm^{-1} .²⁴ And the sample penetration depth of the electron beam can be estimated by the following formulas:²⁵

$$R_e = (0.0276 A / \rho Z^{0.089}) E_b^{1.67} (\mu\text{m}),$$

where ρ is the density of the material ($\rho_{\text{Ge}} = 5.32$ g/cm^3 , $\rho_{\text{GaAs}} = 5.32$ g/cm^3), E_b is the energy (keV) of the electron beam, A is the atomic weight in g/mol, and Z is the atomic number. In our experiment, E_b is equal to 4 keV, $Z_{\text{Ge}} = 32$, $Z_{\text{GaAs}} = 32$ and $A_{\text{Ge}} = 72.59$, $A_{\text{GaAs}} = 72.32$. Thus, we obtain $R_e(\text{Ge}) = 175$ nm, $R_e(\text{GaAs}) = 174$ nm. Thus, the main contribution of CL, in this case, arises from the emission range of the depth near the surface of the samples and peak shifts are decreased.

Another factor influencing the CL spectra may arise from the contamination effect. As the samples were carefully prepared, the contamination effects were minimized and were insignificant. In addition, there is no strong band bending on the cleaned surface (or the band-bending effect is not so strong as to influence the bulk emission). Therefore, the influence of the surface on the measurement results is not important.

In conclusion, by using the CL method, we have observed five structures at 3.05, 3.22, 3.60, 3.90, and 4.30 eV in n -type Ge (111). For lightly doped Ge, it is observed that the band structure does not depend on doping type. For SI GaAs, five structures at 2.95, 3.26, 3.88, 4.28, and 4.96 eV have also been observed. We believe that these CL spectra, which were not apparent in other previous optical studies, are related to the energy band structures of Ge and GaAs.

The authors wish to thank Professor Xia Shang-da and Dr. Li Shu-min for very helpful discussions. The earlier stage of this work was supported by the National Natural Science Foundation of China under Grant No. 19004009.

¹L. Ley *et al.*, Phys. Rev. B **9**, 600 (1974).

²R. H. Williams *et al.*, Rep. Prog. Phys. **43**, 1357 (1980).

³K. Löhnert and E. Kubalek, in *Characterisation of Semiconducting Materials and Devices by EBIC and CL Techniques*, edited by A. G. Cullis *et al.*, IOP Conf. Proc. No. 67 (Institute of Physics and Physical Society, London, 1983), pp. 303–314.

⁴S. Mahajlenko, S. M. Davidson, and B. Hamilton, in *SEM CL Assessment of Minority Carrier Lifetime in Silicon*, edited by A. G. Cullis *et al.*, IOP Conf. Proc. No. 67 (Institute of Physics and Physical Society, London, 1983), pp. 327–332.

⁵M. A. Vouk and E. C. Lightowers, J. Phys. C **10**, 3689 (1977).

⁶H. C. Casey, Jr. and R. H. Kaiser, J. Electrochem. Soc. **114**, 149 (1967).

⁷S. M. Davidson, J. Microsc. (Oxford) **110**, 177 (1977).

⁸M. R. Lorenz and A. Onton, in *Proceedings of the 10th International Conference on the Physics of Semiconductors*, edited by Seymour P. Keller (USAEC, Oak Ridge, 1970), pp. 444–449.

⁹D. A. Cusano, Solid State Commun. **2**, 353 (1964).

¹⁰J. D. Cuthbert and D. G. Thomas, J. Appl. Phys. **39**, 1573 (1968).

¹¹R. A. Smith, *Semiconductors*, 2nd ed. (Cambridge University Press, Cumberpatch, England, 1978), pp. 266 and 366.

¹²M. L. Cohen and T. K. Bergstresser, Phys. Rev. **141**, B789 (1966).

¹³J. R. Chelikowsky and M. L. Cohen, Phys. Rev. B **14**, 556 (1976).

¹⁴T. P. Humphreys and G. P. Srivastava, Phys. Status Solidi B **112**, 581 (1982).

¹⁵B. G. Jacobi and D. B. Holt, J. Appl. Phys. **59**, R1 (1986).

¹⁶B. E. Sernelius, Phys. Rev. B **34**, 5610 (1986).

¹⁷L. Y. Hao *et al.*, Phys. Rev. B **47**, 13 320 (1993).

¹⁸X. L. Xu *et al.*, J. Phys. Condens. Matter **5**, L587 (1993).

¹⁹S. M. Sze, *Physics of Semiconductor Devices* (Wiley, New York, 1981), p. 33, and references therein.

²⁰V. M. Shatalov, O. F. Panchenko, K. N. Pilichak, and E. V. Zolotukhin, Fiz. Tverd. Tela (Leningrad) **31**, 285 (1989) [Sov. Phys. Solid State **31**, 712 (1989)].

²¹H. R. Phillipp and E. A. Taft, Phys. Rev. **113**, 1002 (1959).

²²D. E. Aspnes and A. A. Studna, Phys. Rev. B **27**, 985 (1983).

²³Edward D. Palik, *Handbook of Optical Constants of Solid* (Academic, New York, 1985).

²⁴S. M. Sze, *Physics of Semiconductor Devices* (Ref. 19), p. 42, and references therein.

²⁵K. Kanaya and S. Okayama, J. Phys. D **5**, 43 (1972).